UC Riverside

UC Riverside Previously Published Works

Title

Contribution of Carbonyl Chromophores in Secondary Brown Carbon from Nighttime
Oxidation of Unsaturated Heterocyclic Volatile Organic Compounds.

Chen, Kunpeng

Mayorga, Raphael

Hamilton, Caitlin

et al.

Article

Contribution of Carbonyl Chromophores in Secondary Brown Carbon from Nighttime Oxidation of Unsaturated Heterocyclic Volatile Organic Compounds

Kunpeng Chen, Raphael Mayorga, Caitlin Hamilton, Roya Bahreini, Haofei Zhang, and Ying-Hsuan Lin*

Read Online

ACCESS | Metrics & More | Article Recommendations | SI Supporting Information

ABSTRACT: The light absorption properties of brown carbon (BrC), which are linked to molecular chromophores, may play a significant role in the Earth's energy budget. While nitroaromatic compounds have been identified as strong chromophores in wildfire-driven BrC, other types of chromophores remain to be investigated. Given the electron-withdrawing nature of carbonyls ubiquitous in the atmosphere, we characterized carbonyl chromophores in BrC samples from the nighttime oxidation of furan and pyrrole derivatives, which are important but understudied precursors of secondary organic aerosols primarily found in wildfire emissions. Various carbonyl chromophores were characterized and quantified in BrC samples, and their ultraviolet−visible spectra were simulated by using time-dependent density functional theory. Our findings suggest that chromophores with carbonyls bonded to nitrogen (i.e., imides and amides) derived from N-containing heterocyclic precursors substantially contribute to BrC light absorption. The quantified N-containing carbonyl chromophores contributed to over 40% of the total light absorption at wavelengths below 350 nm and above 430 nm in pyrrole BrC. The contributions of chromophores to total light absorption differed significantly by wavelength, highlighting their divergent importance in different wavelength ranges. Overall, our findings highlight the significance of carbonyl chromophores in secondary BrC and underscore the need for further investigation.

KEYWORDS: *furan and pyrrole derivatives, secondary organic aerosols, imides and amides, light absorption contribution, wavelength dependency*
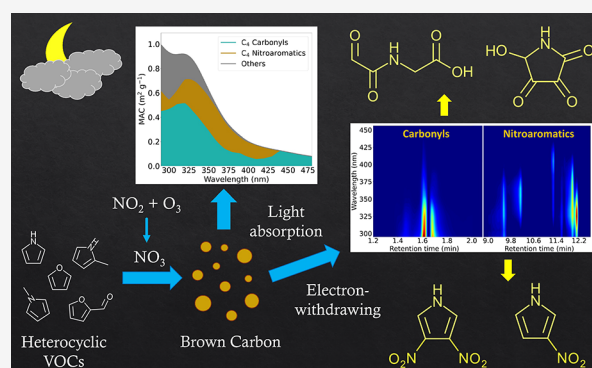
INTRODUCTION

Atmospheric brown carbon (BrC) is an important contributor to global warming, with a $+0.10−0.55$ W m^{-2} direct radiative effect[1−3] ($\sim$20−24% contribution) on the top-of-atmosphere direct radiative forcing.[4,5] The contribution of BrC absorption is enhanced at higher altitudes[6] and varies by both daily and seasonal cycles,[7] especially due to changes in air pollution and cloud coverage.[7,8] Conversely, the light absorption of BrC may also indirectly reduce the global coverage of clouds and decrease their cooling effects.[9] The spatial and temporal variations of BrC light absorption, and consequently their impacts, are strongly related to the changes in chemical composition.[8,10] However, parametrization pertinent to BrC constituents remains underdeveloped in climate models,[11] hindering accurate evaluations of BrC optical properties and climate change prediction.[12,13]

Accurate representations of BrC's effects on climate change require a comprehensive process-level understanding of the formation and evolution of molecular chromophores, which play a key role in regulating the light absorption properties of BrC. Nitroaromatic chromophores, also known as nitrated aromatic compounds, have been recognized as significant contributors to BrC light absorption. For example, Li et al. and Frka et al. reported that nitroaromatic chromophores may contribute to $\sim$17−31% light absorption of BrC at 365−370 nm,[14,15] while Bluvshtein et al. and Lin et al. indicated an even higher ratio (i.e., 50−80%) at wavelengths above 350 nm in biomass burning events.[16,17] Although nitroaromatic chromophores may not account for a large fraction of aerosol mass, their contribution to BrC light absorption at 365 nm can be $\sim$2−10 times that of their mass contribution in BrC samples.[14,15,18,19] Among a variety of nitroaromatic chromophores, nitrophenols and nitrocatechols have been identified as two major groups of nitroaromatic chromophores in ambient

aerosols,[19,20] and they have been widely investigated to characterize the BrC formation and evolution due to photooxidation or photolysis.[21−26]

While nitroaromatic chromophores have been identified as potential tracers of BrC in atmospheric processing due to their significant role in the light absorption of BrC at 365 nm,[27] the contributors to the BrC absorption spectra in the near-ultraviolet (UV) range below 365 nm have not been fully deconvoluted. In contrast to the >50% contribution of light absorption above 350 nm, nitroaromatic chromophores only accounted for ~20% of light absorption at 300 nm in biomass burning events according to studies reported by Bluvshtein et al. and Lin et al.[16,17] The wavelength-dependent contributions to BrC light absorption suggest the critical role of other types of chromophores in UV absorption. Since the light absorption of BrC chromophores is induced by electronic transitions, similar to nitroaromatics, which have strongly electron-withdrawing nitro groups attached to the aromatic rings, unsaturated organic compounds or conjugated systems coupled with other types of electron-withdrawing groups such as carbonyls could also be chromophore candidates.[13,28] For instance, the simplest unsaturated carbonyl compound (i.e., acrolein) can absorb sunlight above 290 nm.[29,30] From field studies, it has been reported that carbonyls may contribute to a large mass fraction of biomass burning aerosols[31,32] and significant light absorption in the BrC.[10,33,34] The molecular absorptivity of numerous carbonyl compounds observed in ambient aerosols is comparable to the absorptivity of nitroaromatic chromophores at 290−350 nm.[35] Therefore, it is essential to characterize carbonyl chromophores and constrain their roles in BrC light absorption.

In this study, we characterized carbonyl chromophores in secondary organic aerosols (SOAs) from the nighttime oxidation of a series of unsaturated heterocyclic volatile organic compounds (VOCs), including pyrrole, 1-methylpyrrole (1-MP), 2-methylpyrrole (2-MP), furan, and furfural, that have been widely observed in biomass burning events[36−40] and may account for ~30% of the initial nitrate radical (NO$_3$) reactivity in wildfire-driven nighttime chemistry.[40] Recently, these VOCs were reported as potentially important precursors for secondary BrC formation during nighttime oxidation,[41−44] in which several carbonyl chromophores were observed.[43] Multi-instrumental characterization along with theoretical calculations of ultraviolet−visible (UV−vis) spectra were employed here to elucidate the structures of carbonyl chromophores and their spectral light absorptivity. This study focuses on the light absorption contribution of carbonyl chromophores in pyrrole SOA and 2-MP SOA; because nitroaromatic chromophores have been identified as critical contributors to BrC light absorption in these systems, they can serve as a benchmark for comparisons.[42] Characterizing BrC chromophores at the molecular level can contribute to a deeper process-level understanding of the formation and evolution of secondary BrC light absorption in changing environments.

■ METHODS

Experimental Setup. Experiments were performed in a 10 m^3 Teflon FEP chamber at room temperature (20−25 °C) and low relative humidity (RH< 20%) in the dark. Details of the experimental setup and SOA properties, including number and size distribution, aerosol effective density, and mass fraction of organics, were introduced in our previous studies.[42,43] In brief,

450 ppb NO$_2$ and 1500 ppb O$_3$ (initial [NO$_2$]/[O$_3$] = 0.3) were first injected into the chamber and allowed to react for 1 h, producing ~22 ppb nitrate radicals (NO$_3$).[42] To investigate the effects of NO$_3$ radical levels on the light absorption contributions of BrC chromophores, additional experiments were carried out with 150 ppb NO$_2$ and 1500 ppb O$_3$ (initial [NO$_2$]/[O$_3$] = 0.1), producing ~8 ppb NO$_3$.[42] The concentrations of NO$_2$ and O$_3$ were monitored by a NO$_x$ analyzer (Teledyne Instruments) and an O$_3$ analyzer (Advanced Pollution Instrumentation, Inc.), respectively. Our previous studies indicated that the nighttime oxidation of pyrroles and furans under both conditions was predominantly initiated by NO$_3$ radicals.[42,44] After the 1 h reaction between O$_3$ and NO$_2$ to produce NO$_3$ radicals, one of the studied heterocyclic VOCs was first vaporized in a heated jar and then injected into the chamber with ~15 lpm of nitrogen gas. The target concentration of VOCs in the chamber was ~200 ppb. After the mass concentration reached a plateau, the generated SOA particles were collected on polytetrafluoroethylene membrane filters (46.2 mm, 2.0 μm, Tisch Scientific) for 1 h with a flow rate of 16.7 lpm; each filter collected the aerosols from 1 m^3 of chamber air and served for subsequent offline analysis. Although chamber experiments have some limitations in simulating the real atmosphere (e.g., size-dependent particulate wall loss rate (Figure S1) that may affect the chromophore quantification),[45] the controlled chamber conditions can systematically facilitate the characterization of carbonyl chromophores and the evaluation of their roles in secondary BrC.

Compositional Analysis. The compositional analysis was conducted by using a suite of complementary analytical instruments. Liquid chromatography coupled with a diode array detector, an electrospray ionization source (negative ion mode), and a quadruple-time-of-flight tandem mass spectrometry (LC-DAD-ESI(-)-Q-TOFMS, Agilent Technologies 1260 Infinity II, and 6545 Q-TOF LC/MS) was used to identify light-absorbing carbonyl products and to characterize their molecular structures. The gradient elution for the changing LC mobile-phase composition over time is shown in Figure S2A. Gas chromatography-electron ionization mass spectrometry (GC/EI-MS, Agilent Technologies 6890N GC System, and 5975 inert XL Mass Selective Detector) was also used to complementarily identify carbonyl products. An iodide-adduct time-of-flight chemical ion mass spectrometer coupled with the filter inlet for gases and aerosols system (FIGAERO-ToF-CIMS, Aerodyne Research Inc.)[46] and an ion mobility spectrometry time-of-flight mass spectrometer (IMS-TOF, Tofwerk Inc.) were used to characterize SOA composition in real time and offline, respectively. All characterization methods were the same as those in our prior studies.[42,43] Detailed instrumental setups and operational parameters have been described previously.[42,43,47−49]

N-containing carbonyl chromophores were characterized by LC-DAD-ESI-Q-TOFMS and GC/EI-MS, and their mass contributions were estimated semiquantitatively using maleimide (C$_4$H$_3$NO$_2$) as a surrogate standard. The mass ratio of the characterized N-containing carbonyl chromophores (MR$_{carbonyl}$) (eq 1) and the mass ratio of maleimide (MR$_{maleimide}$) in SOA samples from pyrrole and its derivatives had been previously determined by GC/EI-MS using a similar approach.[43]
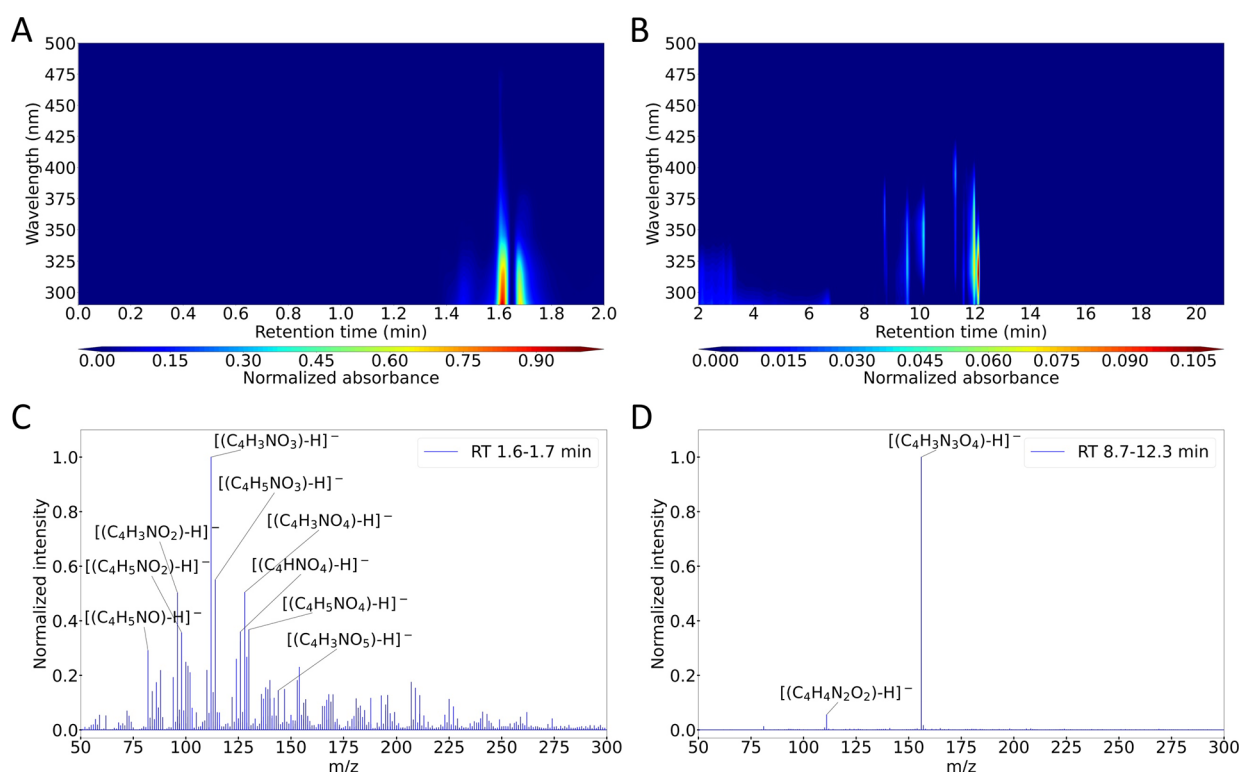
Figure 1. LC-DAD heatmaps of pyrrole SOA: (A) 0−2 min and (B) 2−21 min followed by the mass spectra corresponding to the major hotspots, respectively (C,D). The light absorption of chromophores was normalized to the highest value of the whole LC-DAD heatmap, with each panel having its own color scale for a clear representation of chromophore distribution. With LC mobile phase changing (Figure S2A), the separated hotspots in two unique RT zones represent distinct chromophores with different polarities.

$$\mathrm{MR_{carbonyl}} = \mathrm{MR_{maleimide}} \frac{c_{\mathrm{carbonyl}} M_{\mathrm{carbonyl}}}{c_{\mathrm{maleimide}} M_{\mathrm{maleimide}}}$$

$$= \mathrm{MR_{maleimide}} R_F \frac{A_{\mathrm{carbonyl}} M_{\mathrm{carbonyl}}}{A_{\mathrm{maleimide}} M_{\mathrm{maleimide}}} \quad (1)$$

Here, c_{carbonyl} and $c_{\mathrm{maleimide}}$ are the molar concentrations of the characterized carbonyl chromophores and maleimide in the extracted SOA samples (mol L^{-1}); M_{carbonyl} and $M_{\mathrm{maleimide}}$ are the molar masses of the characterized carbonyl chromophores and maleimide in the extracted SOA samples (g mol^{-1}); A_{carbonyl} and $A_{\mathrm{maleimide}}$ are the peak areas of parent ions of the characterized carbonyl chromophores and maleimide in their extracted ion chromatograms (EICs) measured by LC-DAD-ESI-Q-TOFMS. Although response factors (R_F) of the characterized N-containing carbonyl chromophores may differ slightly from the surrogate standard (Figure S2B), semi-quantification can provide approximate mass ratios and still support comparisons of the representation of various N-containing carbonyl chromophores in SOA samples.

Light Absorption Measurements. The absorbance of the SOA samples (290−700 nm) was measured by a UV−vis spectrophotometer (Beckman DU-640). The SOA mass on each filter sample varied within 10−350 μg depending on the type of VOCs. Each filter sample was extracted with 22 mL of acetonitrile (ACN), which has been shown to be a suitable solvent for the analysis of secondary BrC due to its chemical stability (aprotic) and solubility for polar compounds.[43] It is noted that ACN may not completely extract the SOA constituents from filters (Table S1), so the BrC light absorption estimated in this study is the lower limit. The contribution of BrC carbonyl marker compounds (i.e.,

maleimide and phthalic anhydride)[43] to the total light absorption of SOA samples (AbsC), which can vary greatly with wavelength (λ), is estimated by eq 2.

$$\mathrm{AbsC}(\lambda) = \frac{\mathrm{Abs_{chro}}(\lambda)}{\mathrm{Abs_{BrC}}(\lambda)} \quad (2)$$

$\mathrm{Abs_{BrC}}(\lambda)$ is the total light absorbance of the BrC samples, directly measured by the UV−vis spectrophotometer, while $\mathrm{Abs_{chro}}(\lambda)$ is the light absorbance of the investigated BrC chromophores, calculated by the Beer−Lambert law (eq 3).

$$\mathrm{Abs_{chro}}(\lambda) = \varepsilon_{\mathrm{chro}}(\lambda) \times \frac{m_{\mathrm{chro}}}{M_{\mathrm{chro}}} \times b \quad (3)$$

$\varepsilon_{\mathrm{chro}}(\lambda)$ is the molecular absorptivity of the investigated BrC chromophores (L mol^{-1} cm^{-1}), which has been reported in our previous work;[43] m_{chro} is the mass concentration of molecular chromophores in the SOA solution samples (ng μL^{-1}); M_{chro} is the molar mass of the molecular chromophores (g mol^{-1}); and b is the instrumental light path (i.e., 1 cm).

Computations of Theoretical UV−Vis Spectra. The time-dependent density functional theory was used to simulate the wavelength-dependent light absorptivity of the characterized carbonyl products for which no authentic standards were available. Gaussian 16 program (revision C. 01)[50] was used for all computations with the B3LYP functional[51,52] and the 6-311++G(d,p) basis set[53] as suggested in previous studies.[54,55] The ACN solvent environment was simulated by the integral equation formalism extension of the polarizable continuum model.[56] GaussView 6 program was used to generate the theoretical UV−vis spectra. All of the Cartesian
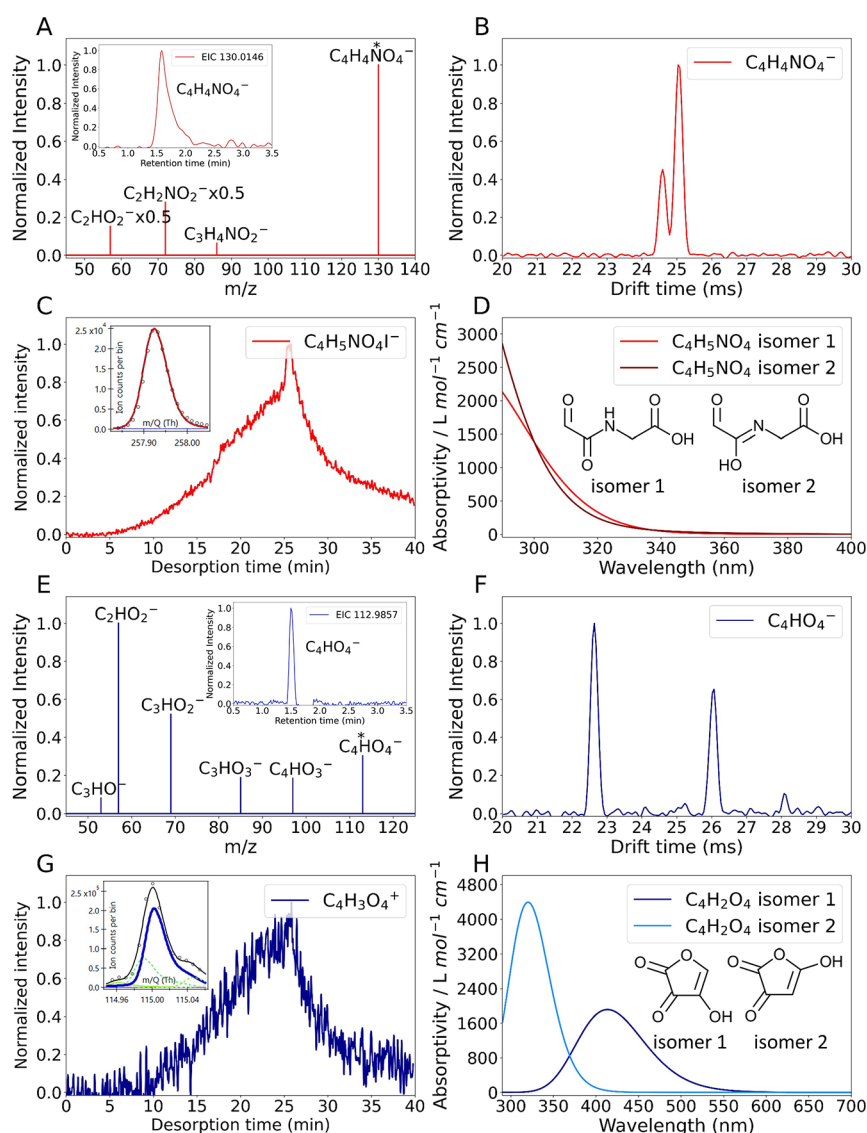
Figure 2. Characterization of carbonyl chromophores in pyrrole SOA and furan SOA: (A) EICs and tandem mass spectra of $C_4H_5NO_4$; (B) IMS-TOF drift grams of $C_4H_5NO_4$; (C) FIGAERO-ToF-CIMS peak fitting and thermograms of $C_4H_5NO_4$; (D) theoretical UV−vis spectra of isomers of $C_4H_5NO_4$; (E) EICs and tandem mass spectra of $C_4H_2O_4$; (F) IMS-TOF drift grams of $C_4H_2O_4$; (G) FIGAERO-ToF-CIMS peak fitting and thermograms of $C_4H_2O_4$ isomers.

coordinates for geometrical structures are summarized in Table S2.

RESULTS AND DISCUSSION

Distribution of Chromophores in the LC-DAD Heatmaps. The LC-DAD heatmaps provide a snapshot of BrC chromophore distributions for all SOA samples (Figure 1 and S3−S5), where the hotspots illustrate the retention time (RT) and wavelengths of light absorption. Figure 1 shows the LC-DAD heatmap of pyrrole SOA, which is divided into two panels corresponding to the RT ranges of 0−2 and 2−21 min (Figure 1A,B).

Compositional analysis revealed that the major hotspots detected at the RT of 1.6−1.7 min may be attributed to mononitrogen chromophores (Figure 1C), while those detected at the RT of 8.7−12.3 min may be ascribed to the dinitrogen and trinitrogen chromophores (Figure 1D). Notably, the analytes at the RT of 1.6−1.7 min comprised many mononitrogen compounds, while only two products

were shown at the RT of 8.7−12.3 min. The mononitrogen chromophores (Figure 1A) in pyrrole SOA collectively acquired much stronger light absorption compared to dinitrogen and trinitrogen chromophores (Figure 1B), which indicated the potential importance of the mononitrogen chromophores in BrC light absorption. The strong light absorption corresponding to mononitrogen chromophores is also observed in 1-MP SOA (Figure S3) and 2-MP SOA (Figure S4), wherein the mononitrogen chromophores led to much higher or similar absorption intensities compared to dinitrogen and trinitrogen chromophores. In a recent study, we found dinitrogen and trinitrogen chromophores in pyrrole SOA and 2-MP SOA as nitro- and dinitro-substituted chromophores.[42] This finding suggested that the mononitrogen chromophores would lack nitro groups, and their nitrogen may be inherited from the pyrrole backbones, as evidenced by the structural characterization in the following section. However, in contrast to electron-withdrawing groups such as nitro groups, the nitrogen atom on the pyrrole
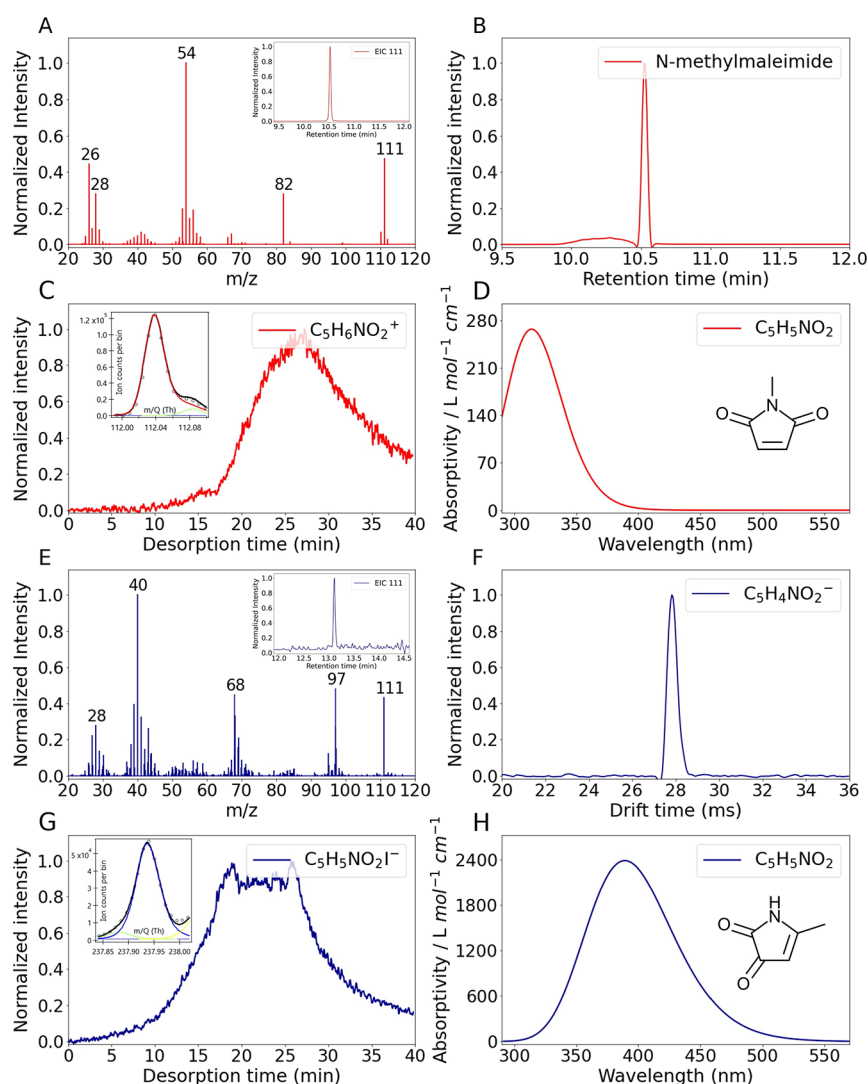
Figure 3. Characterization of carbonyl chromophores in 1-MP SOA and 2-MP SOA: (A) GC/EI-MS characterization of $C_5H_5NO_2$ in 1-MP SOA; (B) EIC of m/z 111 from the N-methylmaleimide chemical standard; (C) FIGAERO-ToF-CIMS peak fitting and thermograms of $C_5H_5NO_2$ in 1-MP SOA; (D) theoretical UV−vis spectrum of $C_5H_5NO_2$ in 1-MP SOA; (E) GC/EI-MS characterization of $C_5H_5NO_2$ in 2-MP SOA; (F) IMS-ToF drift gram of $C_5H_5NO_2$ in 2-MP SOA; (G) FIGAERO-ToF-CIMS peak fitting and thermograms of $C_5H_5NO_2$ in 2-MP SOA; (H) theoretical UV−vis spectrum of $C_5H_5NO_2$ in 2-MP SOA.

backbone cannot attract electron density toward itself, and thus the light absorption of the mononitrogen chromophores is mostly due to the non-nitrogen electron-withdrawing groups in the molecule. Furthermore, our previous study of furan SOA revealed that nitrogen-free products were the predominant contributors to the major LC-DAD hotspots,[44] whereas the major hotspots in furfural SOA can be attributed to both nitrogen-containing and nitrogen-free products (Figure S5). Despite this, all of the LC-DAD heatmaps indicate the importance of different types of electron-withdrawing groups in BrC light absorption. Analysis of functional groups with attenuated total reflectance Fourier-transform infrared spectroscopy conducted in our previous study suggested that chromophores with carbonyl groups may account for a significant portion of the light absorption of SOA samples from nighttime oxidation of heterocyclic VOCs.[43]

Even though nitroaromatic chromophores have been identified as important contributors to BrC light absorption in pyrrole SOA and 2-MP SOA,[41,42] the LC-DAD heatmaps (Figures 1A,B and S3A,B) disclosed that mononitrogen

chromophores could account for the majority of the light absorption. This is because nitroaromatic chromophores and mononitrogen chromophores have absorption peaks at different wavelength ranges and, as a result, have wavelength-dependent light absorption contributions, which will be discussed further in the following sections.

Molecular Characterization of Carbonyl Chromophores. In this study, the molecular composition of carbonyl chromophores was determined by complementary analytical instrumentation, and their UV−vis spectra were simulated using quantum chemical approaches (Figures 2 and 3). Following the identification of the molecular formula in Figure 1C, we performed tandem MS experiments to elucidate their structures. Here, $C_4H_4NO_4^-$, a deprotonated ion of $C_4H_5NO_4$, is selected as an example. The LC-ESI-Q-ToFMS measurements showed a single peak in the EIC of this ion as well as its fragmentation pattern (Figure 2A), which can help derive tentative molecular structures and thus support the theoretical computation of UV−vis spectra. The IMS-TOF measurements also confirmed the presence of $C_4H_4NO_4^-$ in ESI (−) and
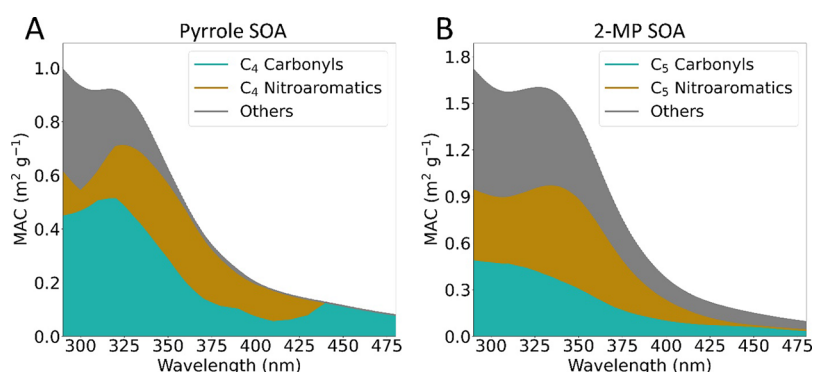
Figure 4. Light absorption contribution of chromophores to MAC profiles: (A) C_4 carbonyls, C_4 nitroaromatics, and other chromophores in pyrrole SOA; (B) C_5 carbonyls, C_5 nitroaromatics, and other chromophores in 2-MP SOA.

indicated two major isomers for this ion (Figure 2B). To rule out the potential interference from the solvent and LC electrospray ionization efficiency,[43,44] the presence of $C_4H_5NO_4$ was supplementally verified by in situ characterization with FIGAERO-ToF-CIMS (Figure 2C). Plausible fragmentation pathways were derived based on the tandem MS data (Figure S6A), wherein $C_4H_5NO_4$ can be characterized as formyl carbonyl amino acetic acid and its imidic acid isomer. Both compounds are chain-structural carbonyl chromophores, as confirmed by the theoretical computation of their UV−vis spectra (Figure 2D). Using the same approaches, the ring-retaining carbonyl chromophores in pyrrole SOA were also characterized, including 2-hydroxy-2-pyrroline-4,5-dione ($C_4H_3NO_3$), 5-hydroxy-2,3,4-pyrrolidinetrione ($C_4H_3NO_4$), and 5-hydroxy-2,3-pyrrolidinedione ($C_4H_5NO_3$) (Figures S7−S10). Similar to the case for pyrrole, nighttime oxidation of furan can generate light-absorbing diones. As one of the major products in furan SOA, $C_4H_2O_4$ was characterized as 4-hydroxyfuran-2,3-dione and 5-hydroxyfuran-2,3-dione (Figures 2E−G and S6B).[44] These products exhibit distinct UV−vis spectra with different central wavelengths and peak absorptivity (Figure 2H).

Given that both LC-ESI-Q-TOFMS and IMS-TOF in this study could detect only deprotonated ions (because of the nature and limitations of ESI(−)) and may not characterize all carbonyls generated, GC/EI-MS was used to investigate more diverse carbonyl chromophores. Previous GC/EI-MS analysis of secondary BrC samples revealed a number of light-absorbing heterocyclic diones, including maleimide (from pyrrole and its derivatives), maleic anhydride, and phthalic anhydride (from furan and furfural).[43] In the current study, *N*-methylmaleimide was discovered by GC/EI-MS (RT = 10.5 min) in 1-MP SOA samples (Figure 3A). The presence of this compound was confirmed by its authentic chemical standard (Figure 3B) and supported by tentative fragmentation pathways (Figure S11A) as well as the in situ FIGAERO-ToF-CIMS measurement (Figure 3C). Also, the presence of 2-methyl-2-pyrroline-4,5-dione, an isomer of *N*-methylmaleimide, in 2-MP SOA was confirmed by multi-instrumental measurements (Figure 3E−G) and the tentative fragmentation pathways (Figure S11B). The calculated UV−vis spectra showed that both diones can contribute to light absorption above 290 nm (Figure 3D,H).

Notably, N-containing carbonyl chromophores such as imides and amides are ubiquitous in SOA samples from N-containing heterocyclic VOC precursors (e.g., pyrrole and its derivatives in this study). The lone pair electrons from the nitrogen atom in imides and amides can conjugate with the

unsaturated bonds (e.g., carbonyl groups), which facilitate the n-π^* excitation of delocalized electrons and hence support the formation of BrC chromophores. However, different N-containing carbonyl chromophores may lead to different contributions to BrC light absorption depending on their mass ratio in SOA samples, spectral wavelengths, and absorptivity. For example, $C_4H_5NO_4$ and $C_4H_3NO_3$ have similar mass ratios in pyrrole SOA (3.37 ± 0.11 and 2.86 ± 0.57%, respectively) based on the semiquantification, but the UV−vis spectrum of $C_4H_5NO_4$ only covers 290−350 nm (Figure 2D), while the UV−vis spectrum of $C_4H_3NO_3$ can extend to 500 nm (Figure S7J). Although the UV−vis spectra of $C_4H_3NO_3$ and $C_4H_3NO_4$ cover a similar range of wavelengths, the latter possesses a higher mass ratio (8.86 ± 1.11%) and lower absorptivity (Figure S7K). It is also noted that the presence of nitrogen may lead to a redshift of the spectral peaks (e.g., Figure S7J and isomer 2 in Figure 2H), suggesting the potentially important role of N-containing carbonyl chromophores in modulating BrC light absorption.

Light Absorption Contribution of Carbonyl and Nitroaromatic Chromophores. The light absorption contributions of identified carbonyl and nitroaromatic chromophores can be estimated by comparing their integrated LC-DAD absorbance within the corresponding RT ranges to the overall LC-DAD absorbance, which are similar to those described in the literature.[16,17] Although the estimated light absorption contributions may not be rigorously accurate due to the incomplete elution of chromophores that can strongly interact with the stationary phase of the LC column,[17] this approach has successfully revealed the indispensable role of nitroaromatic chromophores in BrC aerosols from biomass burning events.[16,17] Similarly, the relative importance of carbonyl chromophores and nitroaromatic chromophores at different wavelengths can thus be evaluated by this approach. Here, C_4 carbonyls and C_4 nitroaromatics in pyrrole SOA, which may predominantly contribute to the major hotspots in the LC-DAD heatmaps (Figure 1), were categorized as two groups of chromophores, while other chromophores, which may comprise oxidation products with higher molecular weights and high double bond equivalence (DBE) (Figure S12), were classified as "others." It is noted that the C_4 N-containing carbonyls (both ring-retaining and ring-opening products) and C_4 nitroaromatics are produced from the C_4 backbone of pyrrole; in other VOC systems, the carbon number of the lower-molecular-weight chromophores can be different and dependent on the VOC precursors. The light absorption contribution of each group of chromophores was
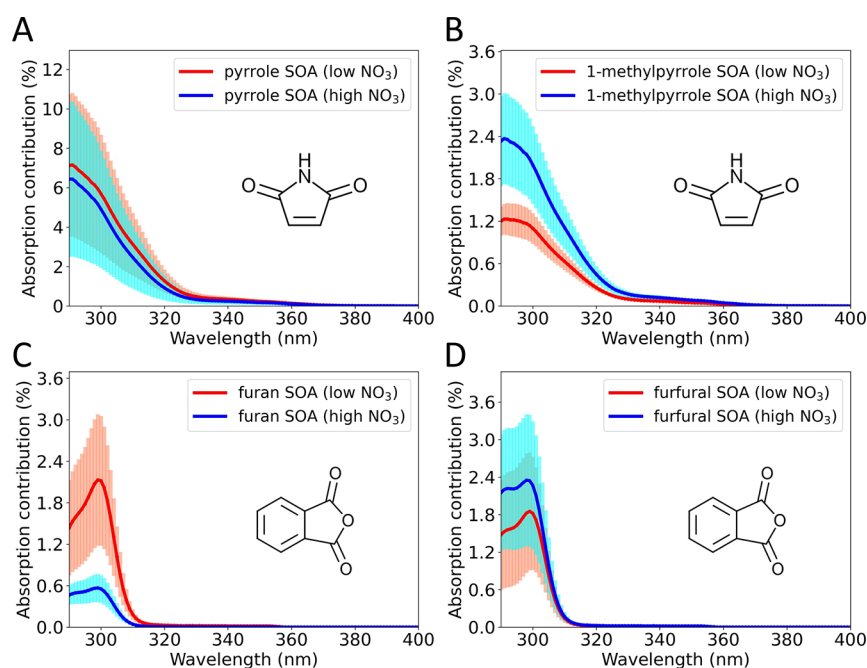
Figure 5. Light absorption contributions of maleimide to (A) pyrrole SOA and (B) 1-MP SOA and phthalic anhydride to (C) furan SOA and (D) furfural SOA under low and high NO_3 levels. The absorption contribution is estimated by the ratio of light absorption of molecular chromophores calculated by the Beer−Lambert law and the total light absorption of BrC samples. The shadow around the lines shows the standard deviation of the absorption contribution at each wavelength.

visualized, along with the wavelengths in both percentages (Figure S13A,B) and mass absorption coefficient (MAC) profiles (Figure 4). The latter was estimated by combining Figure S13 and the MAC profiles reported in our prior study.[42]

Our results showed that, while C_4 nitroaromatics account for the majority of light absorption in the 350−430 nm range, C_4 carbonyls contribute significantly more below 350 nm and above 430 nm, accounting for over 40% of the total light absorption in both wavelength ranges (Figures 4A and S13A). The C_5 nitroaromatics and C_5 carbonyls in 2-MP SOA, which are produced from the C_5 backbone of 2-MP (ref 42 and Figure 3H), revealed comparable tendencies in the wavelength dependence of light absorption contribution (Figures 4B and S13B). However, in the visible range, the contribution of C_4 carbonyls to light absorption was greater than the other two categories in pyrrole SOA (Figures 4A and S13A), whereas the contributions of the three categories in 2-MP SOA were comparable (Figures 4B and S13B). The quantitative differences between Figure 4A and Figure 4B (also between Figure S13A and Figure S13B) reveal the vital role of VOC structures in regulating the relative contributions of carbonyl chromophores and nitroaromatic chromophores to secondary BrC light absorption, which could be due to the interference of diverse oxidation pathways (e.g., diverse pyrrolyl radical shifts).[42]

The relative impact of carbonyl chromophores on BrC light absorption is further evaluated by the ratio of their absorption cross-section emission factors (EF_{absC}), which accounts not only for the MACs but also the carbon emission factors of VOC precursors from burning sources and the SOA yields.[41] Details of the EF_{absC} calculations for pyrrole SOA and 2-MP SOA were described previously.[42] Taking biomass burning of ponderosa pine forests, which is relevant to wildfires in the western US and Canada,[57] as an example, $C_{4−5}$ carbonyl chromophores may contribute more to BrC light absorption

below 350 nm and above 430 nm than $C_{4−5}$ nitroaromatic chromophores (Table S3). It is also noted that the light absorption of 1-MP SOA was mainly attributed to mono-nitrogen $C_{4−5}$ carbonyls and the "others" category instead of $C_{4−5}$ nitroaromatics (Figures 3D, S4, S14A, and S15A). As highlighted in our prior study,[42] the absence of $C_{4−5}$ nitroaromatics may account for the inhibited nitro-substitution by the methyl group on the nitrogen atom of the 1-MP backbone, which reinforces the importance of VOC structures in the light absorption contribution of carbonyl chromophores.

In addition, the heteroatoms in heterocyclic VOCs may greatly alter the oxidation pathways and hence the light absorption contribution of carbonyl and nitroaromatic chromophores. For example, formation of pyrrole-derived nitroaromatics is initiated by the H-abstraction on the nitrogen heteroatom,[42] while formation of furan-derived carbonyls is related to the NO_3 addition and subsequent NO_2 elimination mechanisms affected by the oxygen heteroatom.[58] Our previous research and the current findings suggest that the light absorption of furan SOA can be primarily attributed to $C_{4−5}$ carbonyls and the "others" category (Figures S14B and S15B).[42,44] Nonaromatic nitrosubstituted carbonyl chromophores, such as $C_4H_3NO_7$ in furan SOA,[44] may also contribute to BrC light absorption. Similarly, light absorption of furfural SOA can be mainly attributed to the carbonyl chromophores (Figures S14C and S15C), which is likely related to the carbonyl functional group in furfural. Collectively, these findings demonstrate the significance of carbonyl chromophores in the light absorption of secondary BrC.

Furthermore, depending on the SOA systems, the light absorption contribution of molecular carbonyl chromophores in secondary BrC may vary under different environmental conditions. The NO_3 radical level has been reported as a critical environmental factor that affects the secondary BrC formation of pyrroles and furans.[42−44] As marker compounds

of secondary BrC from the nighttime oxidation of several unsaturated heterocyclic VOC precursors, maleimide, and phthalic anhydride were selected to investigate the influence of NO$_3$ radical levels on their light absorption contribution, and their molecular light absorptivity and mass ratio in various SOA samples have been experimentally measured in prior studies.[43] Our results indicated that the light absorption contribution of maleimide in pyrrole SOA remained essentially constant as the NO$_3$ radical level increased (Figure 5A), whereas it increased significantly in 1-MP SOA as the nitrate radical level increased (Figure 5B). The light absorption contribution of phthalic anhydride exhibited a divergent trend in furan SOA and furfural SOA as the NO$_3$ radical level increased; specifically, it reduced in furan SOA and was enhanced in furfural SOA (Figure 5C,D). The dependence of light absorption contribution on the level of NO$_3$ radicals may be attributed to the alteration of chemical kinetics and, consequently, the branching ratios of carbonyl chromophores production as the NO$_3$ concentrations change. The effects of VOC types on the contribution of molecular carbonyl chromophores to light absorption should also be noted. Maleimide, for instance, may account for ~7% of light absorption at 290 nm in pyrrole SOA (Figure 5A) but a much lower value in 1-MP SOA (Figure 5B). The observed discrepancy could be attributed to the methyl group on 1-MP, which could hinder the formation of maleimide and alternatively generate other chromophores (e.g., N-methyl-maleimide, Figure 3D). Thus, the role of carbonyl chromophores in secondary BrC is significantly influenced by complex atmospheric conditions and VOC emissions.

Overall, our results indicate the prevalence of carbonyl chromophores in SOA from the nighttime oxidation of heterocyclic VOCs. The UV−vis spectra of the characterized carbonyl chromophores cover a wider range of wavelengths (i.e., ~290−500 nm) compared to the nitroaromatic chromophores (i.e., ~290−400 nm) characterized in our previous studies,[42,55] suggesting their distinct contributions to BrC light absorption at different wavelengths. Comparison between isomers also highlights that the spectral light absorptivity of carbonyl chromophores in secondary BrC can be governed by the structure of VOC precursors, which is consistent with our previous research on nitroaromatic chromophores.[42] The structural dependence of UV−vis spectra indicates the importance of structure-related information in the process-level prediction of secondary BrC formation. Moreover, the characterized carbonyl chromophores and their structural analogues, including heterocyclic diones and triones, have been widely observed in SOA systems from other VOCs, for example, those generated by photo-oxidation of a variety of aromatic hydrocarbons.[59−63] Heterocyclic diones have also been widely observed in field measurements of ambient aerosols from biomass burning plumes.[38,64,65] Although triones in ambient aerosols were less reported,[66] they have been suggested as possible contributors to BrC generated from aqueous-phase reactions.[67,68] The collective evidence demonstrates that carbonyl chromophores are ubiquitous constituents of SOA and may play an active role in secondary BrC formation.

■ ATMOSPHERIC IMPLICATIONS

Molecular chromophores are the key to BrC light absorption, connecting the microscopic physicochemical processes in atmospheric aerosols with the macroscopic radiative budget in the Earth system. The newly characterized chromophores enable a more detailed process-level depiction of BrC formation, which is essential for improving the assessment of the impact of BrC in the context of climate change. Our study shows that carbonyl chromophores can be important constituents of secondary BrC from nighttime oxidation of heterocyclic VOCs, with wavelengths ranging from UV to visible. While research on ambient aerosols in wildfires has suggested that nitroaromatic chromophores, such as nitro-phenols, nitrocatechols, nitroguaiacols, and nitrosyringols, may predominantly contribute to BrC light absorption in the visible range,[16,17] field studies have also provided increasing evidence indicating that carbonyl chromophores could be distinct contributors to BrC light absorption in the UV range.[69] It is further noted that the carbonyl chromophores characterized in our studies are not only found in other SOA systems but are also commonly observed in field studies.[38,59−65] Indeed, carbonyl compounds are ubiquitous in atmospheric aerosols and have long been recognized as the key species in tropospheric chemistry[70,71] and the critical precursors of secondary BrC formation in the aerosol phase via NH$_3$/amine-driven reactions[72−75] or forming charge-transfer complexes with alcohols.[76,77] Our study can complementarily provide a new perspective for evaluating the role of carbonyls in atmospheric aerosols based on their intrinsic light absorption, for example, the initiation of photosensitization which can facilitate aqueous SOA formation.[78−82]

Furthermore, carbonyl chromophores produced by the nighttime oxidation of N-containing VOCs may represent a potentially important component in secondary BrC that was previously unrecognized. Our study reveals that light-absorbing imides and amides can be critical chromophores in the SOA of pyrrole and its derivatives. Given that biomass burning releases a variety of N-containing heterocyclic VOC precursors,[37−39] the formation of N-containing carbonyl chromophores could be a potentially significant contributor to the light absorption of secondary BrC. Furthermore, as widely observed in field studies of wildfire emissions,[33,38,83,84] N-containing carbonyl chromophores offer another pivot in addition to the nitro-aromatic chromophores for a more in-depth understanding of secondary BrC formation, particularly the wavelength-dependent change of BrC light absorption as well as the diverse physicochemical processes. Although nitroaromatic chromophores may likely possess stronger absorptivity compared to carbonyl chromophores, the former are largely related to anthropogenic emissions of NO$_x$,[85,86] whereas the latter may be generated by more divergent atmospheric oxidation pathways, such as OH-driven oxidation of VOCs.[64] Broader sources of carbonyl chromophores may result in greater ubiquity in the atmosphere under different environmental conditions, implying more extensive effects. Further research is needed to reveal the role of carbonyl chromophores in other BrC systems and to estimate the radiative forcing from carbonyl chromophores. Overall, this study expands the current understanding of chromophore formation and provides a molecular-level foundation as the basis for further investigations into the effects of secondary BrC formation on Earth's energy budget in the context of climate change.

■ ASSOCIATED CONTENT

ⓈI Supporting Information

The Supporting Information is available free of charge at https://pubs.acs.org/doi/10.1021/acs.est.3c08872.

ACN extraction efficiency of surrogate standards of BrC chromophores; cartesian coordinates for geometrical structures of carbonyl chromophores in the theoretical calculations; wavelength-dependent EF_{absC} of C_{4-5} carbonyls and C_{4-5} nitroaromatics; first-order wall loss rate constants along with particulate diameter; LC mobile-phase composition along with RT and response factors of selected N-containing carbonyls; LC-DAD heatmap and compositional mass spectra of 2-MP SOA; LC-DAD heatmaps and compositional mass spectra of 1-MP SOA; LC-DAD heatmaps and compositional mass spectra of furfural SOA; tentative fragmentation pathways of $C_4H_4NO_4^-$ and $C_4HO_4^-$; heterocyclic carbonyl chromophores in pyrrole SOA; tentative fragmentation pathways of $C_4H_2NO_3^-$; tentative fragmentation pathways of $C_4H_2NO_4^-$; tentative fragmentation pathways of $C_4H_4NO_3^-$; tentative fragmentation pathways of $C_5H_5NO_2$; oxidation products with higher molecular weights and high DBE; light absorption contributions of chromophores in pyrrole SOA and 2-MP SOA in percentages; light absorption contributions of chromophores in 1-MP SOA, furan SOA, and furfural SOA in percentages; and light absorption contributions of chromophores to the MAC profiles in 1-MP SOA, furan SOA, and furfural SOA (PDF)

AUTHOR INFORMATION

Corresponding Author

Ying-Hsuan Lin − *Department of Environmental Sciences, University of California, Riverside, California 92521, United States;* ⦿ orcid.org/0000-0001-8904-1287; Phone: +1-951-827-3785; Email: ying-hsuan.lin@ucr.edu

Authors

Kunpeng Chen − *Department of Environmental Sciences, University of California, Riverside, California 92521, United States;* ⦿ orcid.org/0000-0002-9430-9257

Raphael Mayorga − *Department of Chemistry, University of California, Riverside, California 92521, United States*

Caitlin Hamilton − *Department of Chemistry, University of California, Riverside, California 92521, United States*

Roya Bahreini − *Department of Environmental Sciences, University of California, Riverside, California 92521, United States;* ⦿ orcid.org/0000-0001-8292-5338

Haofei Zhang − *Department of Chemistry, University of California, Riverside, California 92521, United States;* ⦿ orcid.org/0000-0002-7936-4493

Complete contact information is available at:
https://pubs.acs.org/10.1021/acs.est.3c08872

Notes

The authors declare no competing financial interest.

ACKNOWLEDGMENTS

REFERENCES

(1) Lin, G.; Penner, J. E.; Flanner, M. G.; Sillman, S.; Xu, L.; Zhou, C. Radiative forcing of organic aerosol in the atmosphere and on snow: Effects of SOA and brown carbon. *J. Geophys. Res. Atmos.* **2014**, *119* (12), 7453−7476.

(2) Feng, Y.; Ramanathan, V.; Kotamarthi, V. R. Brown carbon: a significant atmospheric absorber of solar radiation? *Atmospheric chemistry and physics* **2013**, *13* (17), 8607−8621.

(3) Zhang, A.; Wang, Y.; Zhang, Y.; Weber, R. J.; Song, Y.; Ke, Z.; Zou, Y. Modeling the global radiative effect of brown carbon: a potentially larger heating source in the tropical free troposphere than black carbon. *Atmos. Chem. Phys.* **2020**, *20* (4), 1901−1920.

(4) Liu, J.; Scheuer, E.; Dibb, J.; Ziemba, L. D.; Thornhill, K. L.; Anderson, B. E.; Wisthaler, A.; Mikoviny, T.; Devi, J. J.; Bergin, M.; Weber, R. J. Brown carbon in the continental troposphere. *Geophys. Res. Lett.* **2014**, *41* (6), 2191−2195.

(5) Zhang, Y.; Forrister, H.; Liu, J.; Dibb, J.; Anderson, B.; Schwarz, J. P.; Perring, A. E.; Jimenez, J. L.; Campuzano-Jost, P.; Wang, Y.; Nenes, A.; Weber, R. J. Top-of-atmosphere radiative forcing affected by brown carbon in the upper troposphere. *Nature Geoscience* **2017**, *10* (7), 486−489.

(6) Zhao, S.; Qi, S.; Yu, Y.; Kang, S.; Dong, L.; Chen, J.; Yin, D. Measurement report: Contrasting elevation-dependent light absorption by black and brown carbon: lessons from in situ measurements from the highly polluted Sichuan Basin to the pristine Tibetan Plateau. *Atmos. Chem. Phys.* **2022**, *22* (22), 14693−14708.

(7) Ferrero, L.; Močnik, G.; Cogliati, S.; Gregorič, A.; Colombo, R.; Bolzacchini, E. Heating Rate of Light Absorbing Aerosols: Time-Resolved Measurements, the Role of Clouds, and Source Identification. *Environ. Sci. Technol.* **2018**, *52* (6), 3546−3555.

(8) Tian, P.; Liu, D.; Zhao, D.; Yu, C.; Liu, Q.; Huang, M.; Deng, Z.; Ran, L.; Wu, Y.; Ding, S.; Hu, K.; Zhao, G.; Zhao, C.; Ding, D. In situ vertical characteristics of optical properties and heating rates of aerosol over Beijing. *Atmos. Chem. Phys.* **2020**, *20* (4), 2603−2622.

(9) Brown, H.; Liu, X.; Feng, Y.; Jiang, Y.; Wu, M.; Lu, Z.; Wu, C.; Murphy, S.; Pokhrel, R. Radiative effect and climate impacts of brown carbon with the Community Atmosphere Model (CAM5). *Atmospheric chemistry and physics* **2018**, *18* (24), 17745−17768.

(10) Xu, J.; Hettiyadura, A. P. S.; Liu, Y.; Zhang, X.; Kang, S.; Laskin, A. Atmospheric Brown Carbon on the Tibetan Plateau: Regional Differences in Chemical Composition and Light Absorption Properties. *Environmental Science & Technology Letters* **2022**, *9* (3), 219−225.

(11) Liu, D.; He, C.; Schwarz, J. P.; Wang, X. Lifecycle of light-absorbing carbonaceous aerosols in the atmosphere. *npj Clim. Atmos. Sci.* **2020**, *3* (1), 40.

(12) Laskin, A.; Laskin, J.; Nizkorodov, S. A. Chemistry of Atmospheric Brown Carbon. *Chem. Rev.* **2015**, *115* (10), 4335−4382.

(13) Moise, T.; Flores, J. M.; Rudich, Y. Optical Properties of Secondary Organic Aerosols and Their Changes by Chemical Processes. *Chem. Rev.* **2015**, *115* (10), 4400−4439.

(14) Li, X.; Wang, Y.; Hu, M.; Tan, T.; Li, M.; Wu, Z.; Chen, S.; Tang, X. Characterizing chemical composition and light absorption of nitroaromatic compounds in the winter of Beijing. *Atmos. Environ.* **2020**, *237*, No. 117712.

(15) Frka, S.; Šala, M.; Brodnik, H.; Štefane, B.; Kroflič, A.; Grgić, I. Seasonal variability of nitroaromatic compounds in ambient aerosols: Mass size distribution, possible sources and contribution to water-soluble brown carbon light absorption. *Chemosphere* **2022**, *299*, No. 134381.

(16) Bluvshtein, N.; Lin, P.; Flores, J. M.; Segev, L.; Mazar, Y.; Tas, E.; Snider, G.; Weagle, C.; Brown, S. S.; Laskin, A.; Rudich, Y. Broadband optical properties of biomass-burning aerosol and identification of brown carbon chromophores. *J. Geophys. Res. Atmos.* **2017**, *122* (10), 5441−5456.

(17) Lin, P.; Bluvshtein, N.; Rudich, Y.; Nizkorodov, S. A.; Laskin, J.; Laskin, A. Molecular Chemistry of Atmospheric Brown Carbon Inferred from a Nationwide Biomass Burning Event. *Environ. Sci. Technol.* **2017**, *51* (20), 11561−11570.

(18) Xie, M.; Hays, M. D.; Holder, A. L. Light-absorbing organic carbon from prescribed and laboratory biomass burning and gasoline vehicle emissions. *Sci. Rep.* **2017**, *7* (1), 7318.

(19) Li, X.; Hu, M.; Wang, Y.; Xu, N.; Fan, H.; Zong, T.; Wu, Z.; Guo, S.; Zhu, W.; Chen, S.; Dong, H.; Zeng, L.; Yu, X.; Tang, X. Links between the optical properties and chemical compositions of brown carbon chromophores in different environments: Contributions and formation of functionalized aromatic compounds. *Sci. Total Environ.* **2021**, *786*, No. 147418.

(20) Wang, Z.; Zhang, J.; Zhang, L.; Liang, Y.; Shi, Q. Characterization of nitroaromatic compounds in atmospheric particulate matter from Beijing. *Atmos. Environ.* **2021**, *246*, No. 118046.

(21) Zhao, R.; Lee, A. K. Y.; Huang, L.; Li, X.; Yang, F.; Abbatt, J. P. D. Photochemical processing of aqueous atmospheric brown carbon. *Atmos. Chem. Phys.* **2015**, *15* (11), 6087−6100.

(22) Hems, R. F.; Abbatt, J. P. D. Aqueous Phase Photo-oxidation of Brown Carbon Nitrophenols: Reaction Kinetics, Mechanism, and Evolution of Light Absorption. *ACS Earth Space Chem.* **2018**, *2* (3), 225−234.

(23) Braman, T.; Dolvin, L.; Thrasher, C.; Yu, H.; Walhout, E. Q.; O'Brien, R. E. Fresh versus Photo-recalcitrant Secondary Organic Aerosol: Effects of Organic Mixtures on Aqueous Photodegradation of 4-Nitrophenol. *Environmental Science & Technology Letters* **2020**, *7* (4), 248−253.

(24) Wang, Y.; Huang, W.; Tian, L.; Wang, Y.; Li, F.; Huang, D. D.; Zhang, R.; Go Mabato, B. R.; Huang, R.-J.; Chen, Q.; Ge, X.; Du, L.; Ma, Y. G.; Gen, M.; Hoi, K. I.; Mok, K. M.; Yu, J. Z.; Chan, C. K.; Li, X.; Li, Y. J. Decay Kinetics and Absorption Changes of Methoxyphenols and Nitrophenols during Nitrate-Mediated Aqueous Photochemical Oxidation at 254 and 313 nm. *ACS Earth Space Chem.* **2022**, *6* (4), 1115−1125.

(25) Yang, J.; Au, W. C.; Law, H.; Leung, C. H.; Lam, C. H.; Nah, T. pH affects the aqueous-phase nitrate-mediated photooxidation of phenolic compounds: implications for brown carbon formation and evolution. *Environ. Sci.: Process Impacts* **2022**, *25*, 176 DOI: 10.1039/D2EM00004K.

(26) Witkowski, B.; Jain, P.; Gierczak, T. Aqueous chemical bleaching of 4-nitrophenol brown carbon by hydroxyl radicals; products, mechanism, and light absorption. *Atmos. Chem. Phys.* **2022**, *22* (8), 5651−5663.

(27) Xie, M.; Chen, X.; Hays, M. D.; Lewandowski, M.; Offenberg, J.; Kleindienst, T. E.; Holder, A. L. Light Absorption of Secondary Organic Aerosol: Composition and Contribution of Nitroaromatic Compounds. *Environ. Sci. Technol.* **2017**, *51* (20), 11607−11616.

(28) McNeill, V. F. Atmospheric Aerosols: Clouds, Chemistry, and Climate. *Annu. Rev. Chem. Biomol. Eng.* **2017**, *8* (1), 427−444.

(29) Gardner, E. P.; Sperry, P. D.; Calvert, J. G. Photo-decomposition of acrolein in oxygen-nitrogen mixtures. *J. Phys. Chem.* **1987**, *91* (7), 1922−1930.

(30) Magneron, I.; Thévenet, R.; Mellouki, A.; Le Bras, G.; Moortgat, G. K.; Wirtz, K. A Study of the Photolysis and OH-initiated Oxidation of Acrolein and trans-Crotonaldehyde. *J. Phys. Chem. A* **2002**, *106* (11), 2526−2537.

(31) Mayol-Bracero, O. L.; Guyon, P.; Graham, B.; Roberts, G.; Andreae, M. O.; Decesari, S.; Facchini, M. C.; Fuzzi, S.; Artaxo, P. Water-soluble organic compounds in biomass burning aerosols over Amazonia 2. Apportionment of the chemical composition and importance of the polyacidic fraction. *J. Geophys. Res.: Atmos.* **2002**, *107* (D20), LBA 59-1−LBA 59-15.

(32) Garcia-Hurtado, E.; Pey, J.; Borrás, E.; Sánchez, P.; Vera, T.; Carratalá, A.; Alastuey, A.; Querol, X.; Vallejo, V. R. Atmospheric PM and volatile organic compounds released from Mediterranean shrubland wildfires. *Atmos. Environ.* **2014**, *89*, 85−92.

(33) Zhou, Y.; West, C. P.; Hettiyadura, A. P. S.; Pu, W.; Shi, T.; Niu, X.; Wen, H.; Cui, J.; Wang, X.; Laskin, A. Molecular Characterization of Water-Soluble Brown Carbon Chromophores in Snowpack from Northern Xinjiang. *China. Environ. Sci. Technol.* **2022**, *56* (7), 4173−4186.

(34) Desyaterik, Y.; Sun, Y.; Shen, X.; Lee, T.; Wang, X.; Wang, T.; Collett, J. L., Jr Speciation of "brown" carbon in cloud water impacted by agricultural biomass burning in eastern China. *J. Geophys. Res. Atmos.* **2013**, *118* (13), 7389−7399.

(35) Jacobson, M. Z. Isolating nitrated and aromatic aerosols and nitrated aromatic gases as sources of ultraviolet light absorption. *J. Geophys. Res. Atmos.* **1999**, *104* (D3), 3527−3542.

(36) Karl, T. G.; Christian, T. J.; Yokelson, R. J.; Artaxo, P.; Hao, W. M.; Guenther, A. The Tropical Forest and Fire Emissions Experiment: method evaluation of volatile organic compound emissions measured by PTR-MS, FTIR, and GC from tropical biomass burning. *Atmos. Chem. Phys.* **2007**, *7* (22), 5883−5897.

(37) Hatch, L. E.; Luo, W.; Pankow, J. F.; Yokelson, R. J.; Stockwell, C. E.; Barsanti, K. C. Identification and quantification of gaseous organic compounds emitted from biomass burning using two-dimensional gas chromatography−time-of-flight mass spectrometry. *Atmos. Chem. Phys.* **2015**, *15* (4), 1865−1899.

(38) Koss, A. R.; Sekimoto, K.; Gilman, J. B.; Selimovic, V.; Coggon, M. M.; Zarzana, K. J.; Yuan, B.; Lerner, B. M.; Brown, S. S.; Jimenez, J. L.; Krechmer, J.; Roberts, J. M.; Warneke, C.; Yokelson, R. J.; de Gouw, J. Non-methane organic gas emissions from biomass burning: identification, quantification, and emission factors from PTR-ToF during the FIREX 2016 laboratory experiment. *Atmos. Chem. Phys.* **2018**, *18* (5), 3299−3319.

(39) Andreae, M. O. Emission of trace gases and aerosols from biomass burning − an updated assessment. *Atmos. Chem. Phys.* **2019**, *19* (13), 8523−8546.

(40) Decker, Z. C. J.; Zarzana, K. J.; Coggon, M.; Min, K.-E.; Pollack, I.; Ryerson, T. B.; Peischl, J.; Edwards, P.; Dubé, W. P.; Markovic, M. Z.; Roberts, J. M.; Veres, P. R.; Graus, M.; Warneke, C.; de Gouw, J.; Hatch, L. E.; Barsanti, K. C.; Brown, S. S. Nighttime Chemical Transformation in Biomass Burning Plumes: A Box Model Analysis Initialized with Aircraft Observations. *Environ. Sci. Technol.* **2019**, *53* (5), 2529−2538.

(41) Jiang, H.; Frie, A. L.; Lavi, A.; Chen, J. Y.; Zhang, H.; Bahreini, R.; Lin, Y.-H. Brown Carbon Formation from Nighttime Chemistry of Unsaturated Heterocyclic Volatile Organic Compounds. *Environ. Sci. Technol. Lett.* **2019**, *6* (3), 184−190.

(42) Mayorga, R.; Chen, K.; Raeofy, N.; Woods, M.; Lum, M.; Zhao, Z.; Zhang, W.; Bahreini, R.; Lin, Y.-H.; Zhang, H. Chemical Structure Regulates the Formation of Secondary Organic Aerosol and Brown Carbon in Nitrate Radical Oxidation of Pyrroles and Methylpyrroles. *Environ. Sci. Technol.* **2022**, *56* (12), 7761−7770.

(43) Chen, K.; Raeofy, N.; Lum, M.; Mayorga, R.; Woods, M.; Bahreini, R.; Zhang, H.; Lin, Y.-H. Solvent effects on chemical composition and optical properties of extracted secondary brown carbon constituents. *Aerosol Sci. Technol.* **2022**, *56* (10), 917−930.

(44) Chen, K.; Mayorga, R.; Raeofy, N.; Lum, M.; Woods, M.; Bahreini, R.; Zhang, H.; Lin, Y.-H. Effects of Nitrate Radical Levels and Pre-Existing Particles on Secondary Brown Carbon Formation from Nighttime Oxidation of Furan. *ACS Earth Space Chem.* **2022**, *6* (11), 2709−2721.

(45) Ziemann, P. J.; Atkinson, R. Kinetics, products, and mechanisms of secondary organic aerosol formation. *Chem. Soc. Rev.* **2012**, *41* (19), 6582−6605.

(46) Lopez-Hilfiker, F. D.; Mohr, C.; Ehn, M.; Rubach, F.; Kleist, E.; Wildt, J.; Mentel, T. F.; Lutz, A.; Hallquist, M.; Worsnop, D.; Thornton, J. A. A novel method for online analysis of gas and particle composition: description and evaluation of a Filter Inlet for Gases and AEROsols (FIGAERO). *Atmos. Meas. Technol.* **2014**, *7* (4), 983−1001.

(47) Zhang, X.; Zhang, H.; Xu, W.; Wu, X.; Tyndall, G. S.; Orlando, J. J.; Jayne, J. T.; Worsnop, D. R.; Canagaratna, M. R. Molecular characterization of alkyl nitrates in atmospheric aerosols by ion mobility mass spectrometry. *Atmos. Meas. Technol.* **2019**, *12* (10), 5535−5545.

(48) Zhao, Z.; Yang, X.; Lee, J.; Tolentino, R.; Mayorga, R.; Zhang, W.; Zhang, H. Diverse Reactions in Highly Functionalized Organic

Aerosols during Thermal Desorption. *ACS Earth Space Chem.* **2020**, 4 (2), 283−296.

(49) Mayorga, R. J.; Zhao, Z.; Zhang, H. Formation of secondary organic aerosol from nitrate radical oxidation of phenolic VOCs: Implications for nitration mechanisms and brown carbon formation. *Atmos. Environ.* **2021**, 244, No. 117910.

(50) Frisch, M. J.; Trucks, G. W.; Schlegel, H. B.; Scuseria, G. E.; Robb, M. A.; Cheeseman, J. R.; Scalmani, G.; Barone, V.; Petersson, G. A.; Nakatsuji, H.; Li, X.; Caricato, M.; Marenich, A. V.; Bloino, J.; Janesko, B. G.; Gomperts, R.; Mennucci, B.; Hratchian, H. P.; Ortiz, J. V.; Izmaylov, A. F.; Sonnenberg, J. L.; Williams; Ding, F.; Lipparini, F.; Egidi, F.; Goings, J.; Peng, B.; Petrone, A.; Henderson, T.; Ranasinghe, D.; Zakrzewski, V. G.; Gao, J.; Rega, N.; Zheng, G.; Liang, W.; Hada, M.; Ehara, M.; Toyota, K.; Fukuda, R.; Hasegawa, J.; Ishida, M.; Nakajima, T.; Honda, Y.; Kitao, O.; Nakai, H.; Vreven, T.; Throssell, K.; Montgomery, Jr., J. A.; Peralta, J. E.; Ogliaro, F.; Bearpark, M. J.; Heyd, J. J.; Brothers, E. N.; Kudin, K. N.; Staroverov, V. N.; Keith, T. A.; Kobayashi, R.; Normand, J.; Raghavachari, K.; Rendell, A. P.; Burant, J. C.; Iyengar, S. S.; Tomasi, J.; Cossi, M.; Millam, J. M.; Klene, M.; Adamo, C.; Cammi, R.; Ochterski, J. W.; Martin, R. L.; Morokuma, K.; Farkas, O.; Foresman, J. B.; Fox, D. J. *Gaussian 16 Rev. C.01*; Wallingford, CT, 2016.

(51) Becke, A. D. Density-functional exchange-energy approximation with correct asymptotic behavior. *Phys. Rev. A* **1988**, 38 (6), 3098−3100.

(52) Stephens, P. J.; Devlin, F. J.; Chabalowski, C. F.; Frisch, M. J. Ab Initio Calculation of Vibrational Absorption and Circular Dichroism Spectra Using Density Functional Force Fields. *J. Phys. Chem.* **1994**, 98 (45), 11623−11627.

(53) Ditchfield, R.; Hehre, W. J.; Pople, J. A. Self-Consistent Molecular-Orbital Methods. IX. An Extended Gaussian-Type Basis for Molecular-Orbital Studies of Organic Compounds. *J. Chem. Phys.* **1971**, 54 (2), 724−728.

(54) Jacquemin, D.; Perpète, E. A.; Scuseria, G. E.; Ciofini, I.; Adamo, C. TD-DFT Performance for the Visible Absorption Spectra of Organic Dyes: Conventional versus Long-Range Hybrids. *J. Chem. Theory Comput.* **2008**, 4 (1), 123−135.

(55) Chen, J. Y.; Rodriguez, E.; Jiang, H.; Chen, K.; Frie, A.; Zhang, H.; Bahreini, R.; Lin, Y.-H. Time-Dependent Density Functional Theory Investigation of the UV−Vis Spectra of Organonitrogen Chromophores in Brown Carbon. *ACS Earth Space Chem.* **2020**, 4 (2), 311−320.

(56) Mennucci, B.; Cammi, R.; Tomasi, J. Excited states and solvatochromic shifts within a nonequilibrium solvation approach: A new formulation of the integral equation formalism method at the self-consistent field, configuration interaction, and multiconfiguration self-consistent field level. *J. Chem. Phys.* **1998**, 109 (7), 2798−2807.

(57) Veblen, T. T.; Kitzberger, T.; Donnegan, J. Climatic and Human Influences on Fire Regimes in Ponderosa Pine Forests in the Colorado Front Range. *Ecological Applications* **2000**, 10 (4), 1178−1195.

(58) Zhang, W.; Wang, T.; Du, B.; Mu, L.; Feng, C. Mechanism for the gas-phase reaction between NO3 and furan: A theoretical study. *Chem. Phys. Lett.* **2008**, 455 (4), 164−168.

(59) Forstner, H. J. L.; Flagan, R. C.; Seinfeld, J. H. Secondary Organic Aerosol from the Photooxidation of Aromatic Hydrocarbons: Molecular Composition. *Environ. Sci. Technol.* **1997**, 31 (5), 1345−1358.

(60) Yu, J.; Jeffries, H. E.; Sexton, K. G. Atmospheric photooxidation of alkylbenzenes—I. *Carbonyl product analyses. Atmos. Environ.* **1997**, 31 (15), 2261−2280.

(61) Edney, E. O.; Driscoll, D. J.; Weathers, W. S.; Kleindienst, T. E.; Conver, T. S.; McIver, C. D.; Li, W. Formation of Polyketones in Irradiated Toluene/Propylene/NO x/Air Mixtures. *Aerosol Sci. Technol.* **2001**, 35 (6), 998−1008.

(62) Hamilton, J. F.; Lewis, A. C.; Bloss, C.; Wagner, V.; Henderson, A. P.; Golding, B. T.; Wirtz, K.; Martin-Reviejo, M.; Pilling, M. J. Measurements of photo-oxidation products from the reaction of a series of alkyl-benzenes with hydroxyl radicals during EXACT using comprehensive gas chromatography. *Atmos. Chem. Phys.* **2003**, 3 (6), 1999−2014.

(63) Lee, J. Y.; Lane, D. A. Unique products from the reaction of naphthalene with the hydroxyl radical. *Atmos. Environ.* **2009**, 43 (32), 4886−4893.

(64) Coggon, M. M.; Lim, C. Y.; Koss, A. R.; Sekimoto, K.; Yuan, B.; Gilman, J. B.; Hagan, D. H.; Selimovic, V.; Zarzana, K. J.; Brown, S. S.; Roberts, J. M.; Müller, M.; Yokelson, R.; Wisthaler, A.; Krechmer, J. E.; Jimenez, J. L.; Cappa, C.; Kroll, J. H.; de Gouw, J.; Warneke, C. OH chemistry of non-methane organic gases (NMOGs) emitted from laboratory and ambient biomass burning smoke: evaluating the influence of furans and oxygenated aromatics on ozone and secondary NMOG formation. *Atmos. Chem. Phys.* **2019**, 19 (23), 14875−14899.

(65) Liang, Y.; Weber, R. J.; Misztal, P. K.; Jen, C. N.; Goldstein, A. H. Aging of Volatile Organic Compounds in October 2017 Northern California Wildfire Plumes. *Environ. Sci. Technol.* **2022**, 56 (3), 1557−1567.

(66) Edney, E. O.; Kleindienst, T. E.; Conver, T. S.; McIver, C. D.; Corse, E. W.; Weathers, W. S. Polar organic oxygenates in PM2.5 at a southeastern site in the United States. *Atmos. Environ.* **2003**, 37 (28), 3947−3965.

(67) De Haan, D. O.; Jansen, K.; Rynaski, A. D.; Sueme, W. R. P.; Torkelson, A. K.; Czer, E. T.; Kim, A. K.; Rafla, M. A.; De Haan, A. C.; Tolbert, M. A. Brown Carbon Production by Aqueous-Phase Interactions of Glyoxal and SO2. *Environ. Sci. Technol.* **2020**, 54 (8), 4781−4789.

(68) Al-Abadleh, H. A.; Rana, M. S.; Mohammed, W.; Guzman, M. I. Dark Iron-Catalyzed Reactions in Acidic and Viscous Aerosol Systems Efficiently Form Secondary Brown Carbon. *Environ. Sci. Technol.* **2021**, 55 (1), 209−219.

(69) Lin, P.; Aiona, P. K.; Li, Y.; Shiraiwa, M.; Laskin, J.; Nizkorodov, S. A.; Laskin, A. Molecular Characterization of Brown Carbon in Biomass Burning Aerosol Particles. *Environ. Sci. Technol.* **2016**, 50 (21), 11815−11824.

(70) Carlier, P.; Hannachi, H.; Mouvier, G. The chemistry of carbonyl compounds in the atmosphere—A review. *Atmos. Environ.* **1986**, 20 (11), 2079−2099.

(71) Lary, D. J.; Shallcross, D. E. Central role of carbonyl compounds in atmospheric chemistry. *J. Geophys. Res. Atmos.* **2000**, 105 (D15), 19771−19778.

(72) Updyke, K. M.; Nguyen, T. B.; Nizkorodov, S. A. Formation of brown carbon via reactions of ammonia with secondary organic aerosols from biogenic and anthropogenic precursors. *Atmos. Environ.* **2012**, 63, 22−31.

(73) Kampf, C. J.; Jakob, R.; Hoffmann, T. Identification and characterization of aging products in the glyoxal/ammonium sulfate system – implications for light-absorbing material in atmospheric aerosols. *Atmos. Chem. Phys.* **2012**, 12 (14), 6323−6333.

(74) Kampf, C. J.; Filippi, A.; Zuth, C.; Hoffmann, T.; Opatz, T. Secondary brown carbon formation via the dicarbonyl imine pathway: nitrogen heterocycle formation and synergistic effects. *Phys. Chem. Chem. Phys.* **2016**, 18 (27), 18353−18364.

(75) Marrero-Ortiz, W.; Hu, M.; Du, Z.; Ji, Y.; Wang, Y.; Guo, S.; Lin, Y.; Gomez-Hermandez, M.; Peng, J.; Li, Y.; Secrest, J.; Zamora, M. L.; Wang, Y.; An, T.; Zhang, R. Formation and Optical Properties of Brown Carbon from Small α-Dicarbonyls and Amines. *Environ. Sci. Technol.* **2019**, 53 (1), 117−126.

(76) Phillips, S. M.; Smith, G. D. Light Absorption by Charge Transfer Complexes in Brown Carbon Aerosols. *Environ. Sci. Technol. Lett.* **2014**, 1 (10), 382−386.

(77) Phillips, S. M.; Smith, G. D. Further Evidence for Charge Transfer Complexes in Brown Carbon Aerosols from Excitation−Emission Matrix Fluorescence Spectroscopy. *J. Phys. Chem. A* **2015**, 119 (19), 4545−4551.

(78) Smith, J. D.; Sio, V.; Yu, L.; Zhang, Q.; Anastasio, C. Secondary Organic Aerosol Production from Aqueous Reactions of Atmospheric Phenols with an Organic Triplet Excited State. *Environ. Sci. Technol.* **2014**, 48 (2), 1049−1057.

(79) Yu, L.; Smith, J.; Laskin, A.; Anastasio, C.; Laskin, J.; Zhang, Q. Chemical characterization of SOA formed from aqueous-phase reactions of phenols with the triplet excited state of carbonyl and hydroxyl radical. *Atmos. Chem. Phys.* **2014**, *14* (24), 13801−13816.

(80) George, C.; Brüggemann, M.; Hayeck, N.; Tinel, L.; Donaldson, J., Chapter 14 - Interfacial Photochemistry. In *Physical Chemistry of Gas-Liquid Interfaces*; Faust, J. A.; House, J. E., Eds.; Elsevier: 2018; pp 435−457.

(81) Mabato, B. R. G.; Lyu, Y.; Ji, Y.; Li, Y. J.; Huang, D. D.; Li, X.; Nah, T.; Lam, C. H.; Chan, C. K. Aqueous secondary organic aerosol formation from the direct photosensitized oxidation of vanillin in the absence and presence of ammonium nitrate. *Atmos. Chem. Phys.* **2022**, *22* (1), 273−293.

(82) Mabato, B. R. G.; Li, Y. J.; Huang, D. D.; Wang, Y.; Chan, C. K. Comparison of aqueous secondary organic aerosol (aqSOA) product distributions from guaiacol oxidation by non-phenolic and phenolic methoxybenzaldehydes as photosensitizers in the absence and presence of ammonium nitrate. *Atmos. Chem. Phys.* **2023**, *23* (4), 2859−2875.

(83) Permar, W.; Wang, Q.; Selimovic, V.; Wielgasz, C.; Yokelson, R. J.; Hornbrook, R. S.; Hills, A. J.; Apel, E. C.; Ku, I. T.; Zhou, Y.; Sive, B. C.; Sullivan, A. P.; Collett, J. L., Jr; Campos, T. L.; Palm, B. B.; Peng, Q.; Thornton, J. A.; Garofalo, L. A.; Farmer, D. K.; Kreidenweis, S. M.; Levin, E. J. T.; DeMott, P. J.; Flocke, F.; Fischer, E. V.; Hu, L. Emissions of Trace Organic Gases From Western U.S. Wildfires Based on WE-CAN Aircraft Measurements. *J. Geophys. Res. Atmos.* **2021**, *126* (11), No. e2020JD033838.

(84) Hayden, K. L.; Li, S. M.; Liggio, J.; Wheeler, M. J.; Wentzell, J. J. B.; Leithead, A.; Brickell, P.; Mittermeier, R. L.; Oldham, Z.; Mihele, C. M.; Staebler, R. M.; Moussa, S. G.; Darlington, A.; Wolde, M.; Thompson, D.; Chen, J.; Griffin, D.; Eckert, E.; Ditto, J. C.; He, M.; Gentner, D. R. Reconciling the total carbon budget for boreal forest wildfire emissions using airborne observations. *Atmos. Chem. Phys.* **2022**, *22* (18), 12493−12523.

(85) Wang, Y.; Hu, M.; Wang, Y.; Zheng, J.; Shang, D.; Yang, Y.; Liu, Y.; Li, X.; Tang, R.; Zhu, W.; Du, Z.; Wu, Y.; Guo, S.; Wu, Z.; Lou, S.; Hallquist, M.; Yu, J. Z. The formation of nitro-aromatic compounds under high NOx and anthropogenic VOC conditions in urban Beijing. China. *Atmos. Chem. Phys.* **2019**, *19* (11), 7649−7665.

(86) Siemens, K.; Morales, A.; He, Q.; Li, C.; Hettiyadura, A. P. S.; Rudich, Y.; Laskin, A. Molecular Analysis of Secondary Brown Carbon Produced from the Photooxidation of Naphthalene. *Environ. Sci. Technol.* **2022**, *56* (6), 3340−3353.